SUPPLEMENTARY MATERIAL

Ambra1 deficiency impairs mitophagy in skeletal muscle

Lisa Gambarotto *[1,2], Samuele Metti *[1], Martina Chrisam [1], Cristina Cerqua [3], Patrizia Sabatelli [4,5], Andrea Armani [6,7], Carlo Zanon [3], Marianna Spizzotin [2], Silvia Castagnaro [1], Flavie Strapazzon [8], Paolo Grumati [9], Matilde Cescon [1], Paola Braghetta [1], Eva Trevisson [3,11], Francesco Cecconi [12], Paolo Bonaldo [1]

[1] Department of Molecular Medicine, University of Padova, Padova, Italy.

[2] Department of Biology, University of Padova, Padova, Italy.

[3] Institute of Pediatric Research IRP, “Fondazione Città della Speranza”, Padova, Italy.

[4] IRCCS Istituto Ortopedico Rizzoli, Bologna, Italy.

[5] CNR - Institute of Molecular Genetics “Luigi Luca Cavalli-Sforza”, Unit of Bologna, Bologna, Italy.

[6] Department of Biomedical Sciences, University of Padova, Padova, Italy.

[7] Fondazione per la Ricerca Biomedica Avanzata, VIMM, Padova, Italy.

[8] IRCCS Fondazione Santa Lucia, Rome, Italy.

[9] Telethon Institute of Genetics and Medicine, Pozzuoli, Italy.

[10] Department of Clinical Medicine and Surgery, Federico II University, Napoli, Italy.

[11] Clinical Genetics Unit, Department of Women’s and Children’s Health, University of Padova, Padova, Italy.

[12] Danish Cancer Society Research Center, Copenhagen, Denmark.

* These authors contributed equally to this work.

Correspondence should be addressed to P. Bonaldo (bonaldo@bio.unipd.it), Department of Molecular Medicine, University of Padova, Via Ugo Bassi 58/B, 35131 Padova, Italy; Tel.: (+39) 049 827 6084; Fax: (+39) 049 827 6079.

Supplementary Table S1

List of primer sequences used for genotyping or qPCR.

Gene/transgene	Use	Primer	Sequence
FLP	genotyping	FLP For	GAGACAAAGACAAGCGTTAGTAGG
	genotyping	FLP Rev	GTGCGAAGTAGTGATCAGGTATTG
Cre	genotyping	Cre For	CACCAGCCAGCTATCAACTCG
	genotyping	Cre Rev	TTACATTGGTCCAGCCACCAG
Ambra1<tm1a>	genotyping	Neo For	GGGATCTCATGCTGGAGTTCTTCG
	genotyping	tm1c Rev	CTAATCCGCCTACTGCGACT
Ambra1<tm1c>	genotyping	tm1c_d For	TGATAGTCCACGCTCGACCT
	genotyping	tm1c Rev	CTAATCCGCCTACTGCGACT
Ambra1<tm1d>	genotyping	tm1c_d For	TGATAGTCCACGCTCGACCT
	genotyping	tm1d Rev	TGAACATTCCAGCTTGGTGC
Ambra1 (wt)	genotyping	Ambra1 For	TCTGGTTGCCTAGATGGGGA
	genotyping	Ambra1 Rev	ACTCATGTTAGAGCCTCCTGC
Tert	qPCR	TERT For	CTAGCTCATGTGTCAAGACCCTCTT
	qPCR	TERT Rev	GCCAGCACGTTTCTCTCGTT
Nd4	qPCR	ND4 For	AACGGATCCACAGCCGTA
	qPCR	ND4 Rev	AGTCCTCGGGCCATGATT
Ppargc1a	qPCR	PGC1α For	CACCAAACCCACAGAAAACAG
	qPCR	PGC1α Rev	GGGTCAGAGGAAGAGATAAAGTTG
Tfam	qPCR	TFAM For	CACCCAGATGCAAAACTTTCAG
	qPCR	TFAM Rev	CTGCTCTTTATACTTGCTCACAG
Ambra1	qPCR	Ambra1 For	CTGCCTGATAGTCCACGCTC
	qPCR	Ambra1 Rev	TGTGTGGATGCCAAGAGAGTC

Supplementary Table S2

List of antibodies and concentrations used for western blotting (WB) or immunofluorescence (IF).

Primary antibody	Company	cat.n	use	conc
FLAG	Sigma	F1804	WB	1:1000
GAPDH	Millipore	MAB374	WB	1:50000
COX4	Cell Signalling	4844	WB	1:2000
LC3B	Thermo	PA1-169	WB	1:1000
Ambra1	Millipore	ABC131	WB	1:1000
Vinculin	Sigma	V4505	WB	1:2000
Dystrophin	SCBT	sc-15376	IF	1:100
Myosin IIA	DSHB	SC-71-c	IF	1:100
LAMP1	DSHB	1D4B	IF,WB	1:100, 1:1000
TOMM20	SCBT	sc-11415	IF,WB	1:100, 1:1000
DRP1	BD Bioscience	611112	WB	1:1000
PARK2	SCBT	sc-32282	WB	1:1000
SQSTM1	Progen	GP62-C	WB	1:1000
TFAM	Genetex	103231	WB	1:1000
PGC-1α	Abcam	Ab54481	WB	1:1000
Histone-H1	SCBT	sc-10806	WB	1:1000

Supplementary Figure S1

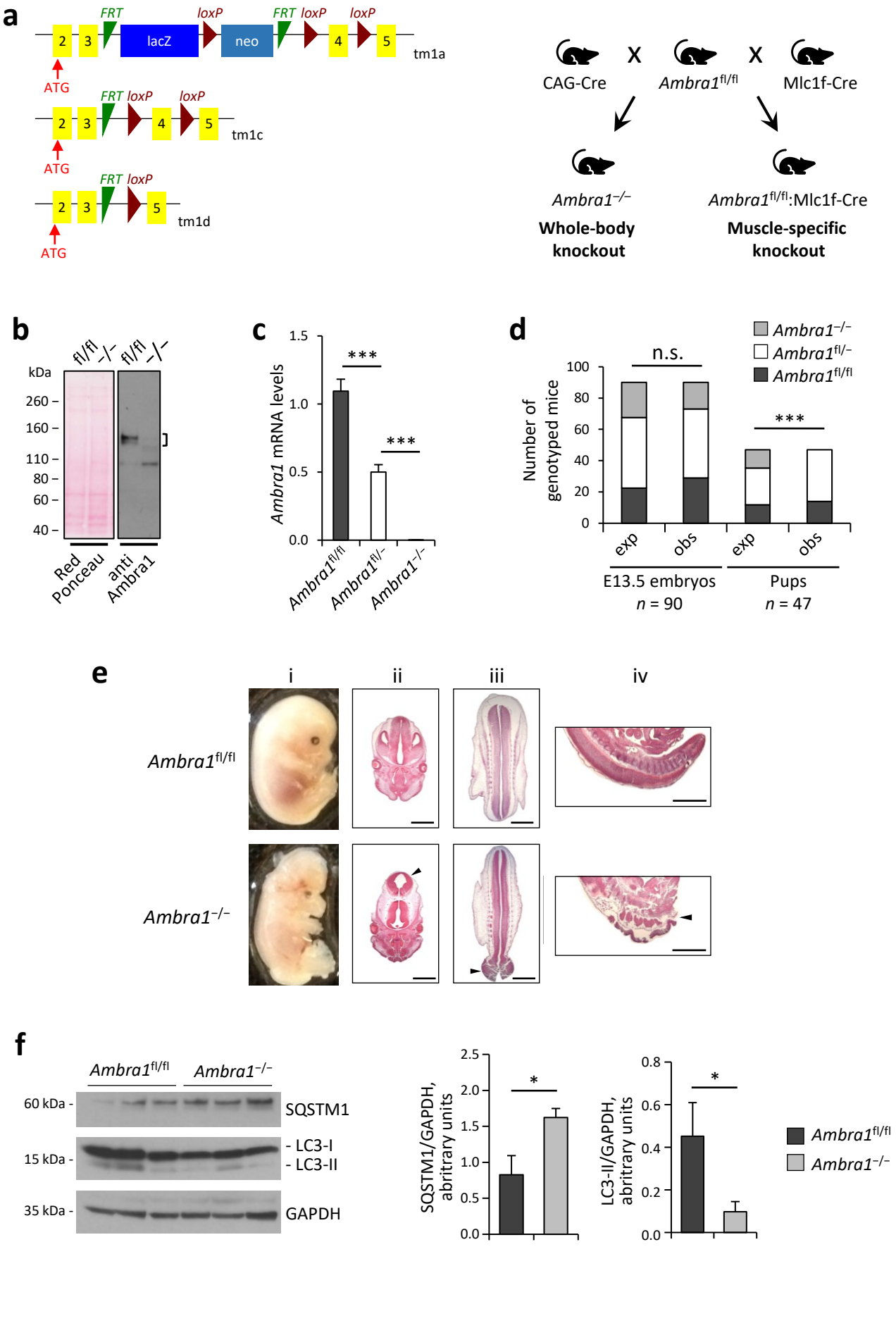

Supplementary Figure S1. Generation and characterization of Ambra1 knockout mice. (**a**) Schematic drawing of the procedure for generation of whole-body and muscle-specific *Ambra1* knockout mice. The *Ambra1* <tm1a(EUCOMM)Wtsi> ("tm1a") construct is made of FRT-flanked *lacZ*/*neo* cassettes inserted in the fourth intron of *Ambra1* gene and followed by one *loxP* site. Two additional *loxP* sites are inserted between *lacZ* and *neo* cassettes and downstream *Ambra1* exon 4, respectively. A conditional *Ambra1* floxed ("tm1c") allele, in which exon 4 is flanked by *loxP* sites, is obtained by FLP recombinase expression. Subsequent Cre expression results in the deletion of exon 4 and generation of a *null* ("tm1d") allele for *Ambra1* gene. Whole-body *Ambra1 null* (*Ambra1*$^{-/-}$) embryos were generated by breeding *Ambra1* floxed (*Ambra1*$^{fl/fl}$) mice with transgenic mice carrying the CAG-Cre transgene, in which Cre expression is driven by a chicken cytomegalovirus immediate early enhancer/chicken beta-actin hybrid promoter, thus allowing for Cre-mediated recombination at the zygote stage. Muscle-specific *Ambra1 null* (*Ambra1*$^{fl/fl}$:*Mlc1f*-Cre) mice were obtained by breeding *Ambra1* floxed (*Ambra1*$^{fl/fl}$) mice with mice carrying the Cre transgene under the control of the *Mlc1f* promoter, which allows for selective expression of Cre recombinase in skeletal muscle. (**b**) Western blotting for Ambra1 in protein extracts derived from whole *Ambra1*$^{fl/fl}$ (fl/fl) and *Ambra1*$^{-/-}$ (–/–) embryos. Ponceau staining served as a loading control. The square bracket indicates the position of Ambra1 signal. (**c**) Quantitative RT-PCR for *Ambra1* mRNA in whole *Ambra1*$^{fl/fl}$, *Ambra1*$^{fl/-}$ and *Ambra1*$^{-/-}$ embryos. Data are shown as mean±s.e.m. (*n* = 4 mice, each genotype; ***, *P*<0.001). (**d**) Genotypic analysis of the progeny of *Ambra1*$^{fl/-}$ mating pairs, as determined at the embryonic stage E13.5 and in newborn pups, comparing expected mendelian genotypes (exp) with the observed genotypes (obs) (***, *P*<0.001; n.s., not significant). (**e**) Phenotypic defects of *Ambra1*$^{-/-}$ E13.5 embryos. From left to right, the respective panels show representative images of: (i) macroscopic appearance of E13.5 *Ambra1*$^{fl/fl}$ and *Ambra1*$^{-/-}$ embryos; (ii) haematoxylin-eosin staining of a frontal section of the head, in which arrowhead points at exencephaly; (iii) haematoxylin-eosin staining of the dorsal region of the trunk, showing enlargement of the caudal part of the neural tube (arrowhead); (iv) haematoxylin-eosin staining of a sagittal section of the caudal region, showing defective closure of the neural tube (arrowhead). Scale bar, 1 mm. (**f**) Western blotting for p62/SQSTM1 and LC3 in protein extracts of *Ambra1*$^{fl/fl}$ and *Ambra1*$^{-/-}$ E13.5 embryos. GAPDH was used as loading control. Densitometric quantifications of SQSTM1 vs GAPDH and of LC3-II vs GAPDH, as determined by at least three independent experiments, are shown on the right panels. Data are shown as mean±s.e.m. (*n* = 4-5 mice, each genotype; *, *P* <0.05).

Supplementary Figure S2

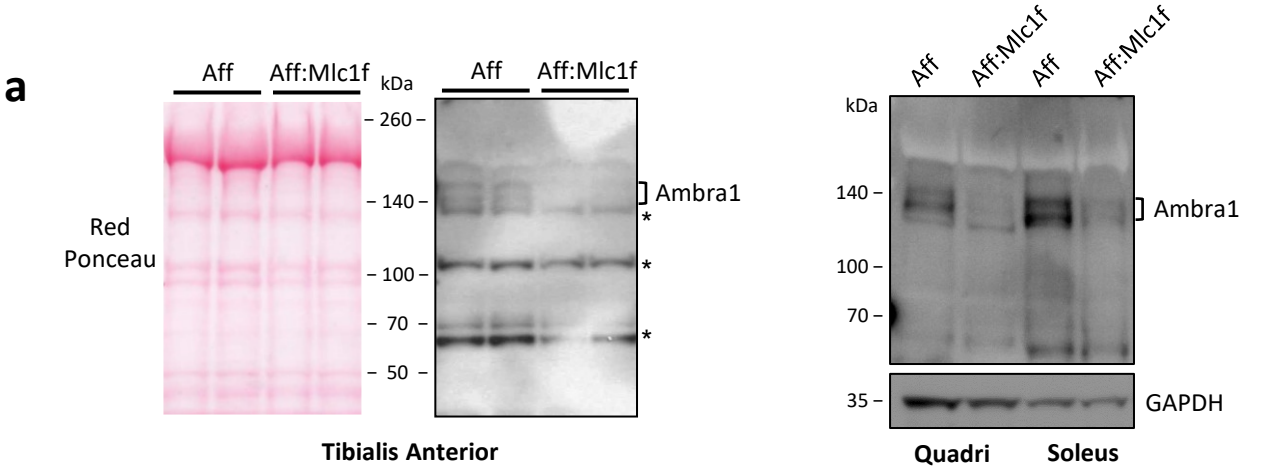

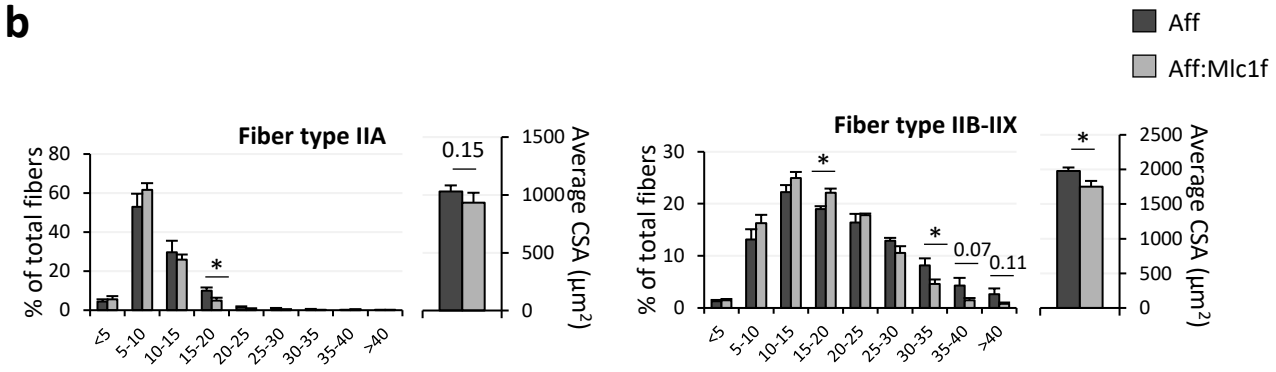

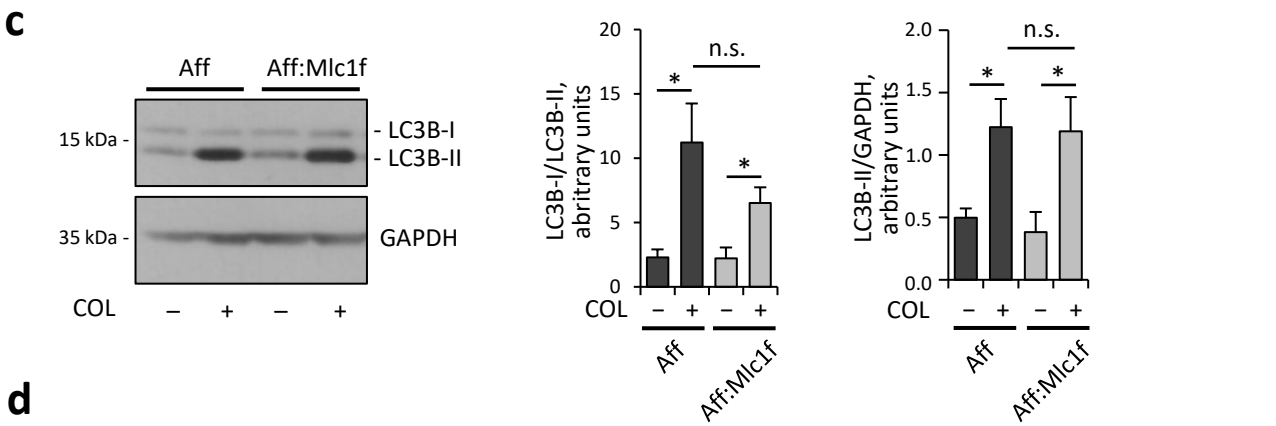

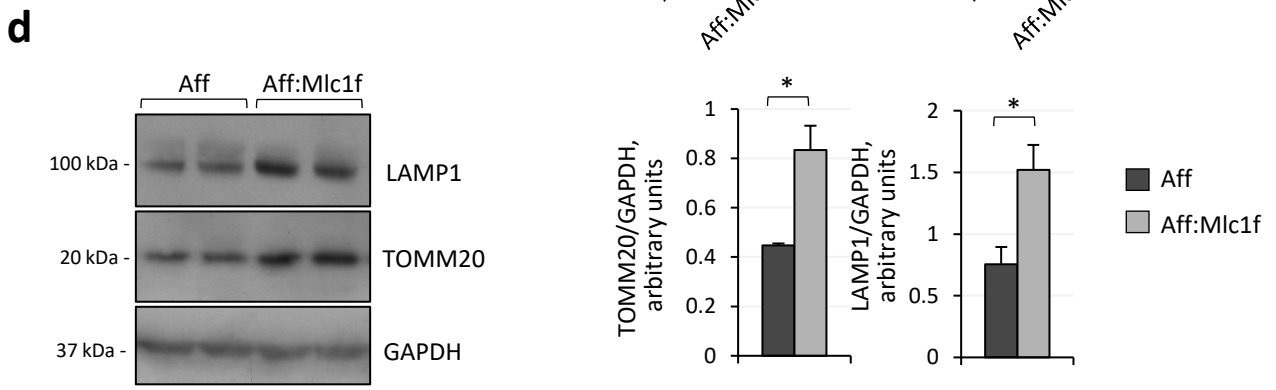

Supplementary Figure S2. Characterization of muscle-specific Ambra1 knockout mice. (**a**) Western blot analysis to confirm correct Ambra1 ablation in different types of skeletal muscles. The panels show representative blotting of protein extracts from tibialis anterior, quadriceps (Quadri) and soleus muscle of *Ambra1*$^{fl/fl}$ (Aff) and *Ambra1*$^{f/f}$:*Mlc1f*-Cre (Aff:Mlc1f) mice. Ponceau staining or GAPDH were used as loading controls. Asterisks mark non-specific bands. (**b**) Morphometric analysis for CSA distribution among myofibers and average cross-sectional area of fiber type IIA (left) and type IIB/IIX (right) of 6-month-old *Ambra1*$^{fl/fl}$ (Aff) and *Ambra1*$^{fl/fl}$::*Mlc1f*-Cre (Aff:Mlc1f) mice. Data are shown as mean±s.e.m. (*n* = 5-6 mice, each genotype; *, *P* <0.05). (**c**) Representative western blotting for LC3 in TA muscle protein extract from 6-month-old *Ambra1*$^{fl/fl}$ (Aff) and *Ambra1*$^{fl/fl}$::*Mlc1f*-Cre (Aff:Mlc1f) mice, treated (+) or not (-) with colchicine (COL). GAPDH was used as loading control. Densitometric quantifications of LC3-I vs LC3-II and of LC3-II vs GAPDH, as determined by at least three independent experiments, are shown on the right panels. Data are shown as mean±s.e.m. (*n* = 6-7 mice, each condition; *, *P* <0.05; n.s., not significant). (**d**) Western blotting for LAMP1 and TOMM20 in protein extract of TA muscle from 6-month-old *Ambra1*$^{f/f}$ (Aff) and *Ambra1*$^{f/f}$:*Mlc1f*-Cre (Aff:Mlc1f-Cre) mice. GAPDH was used as loading control. Densitometric quantifications of LAMP1 vs GAPDH and of TOMM20 vs GAPDH are shown on the right panels. Data are provided as mean±s.e.m. (*n* = 4-6 mice, each genotype; *, *P* <0.05).

Supplementary Figure S3

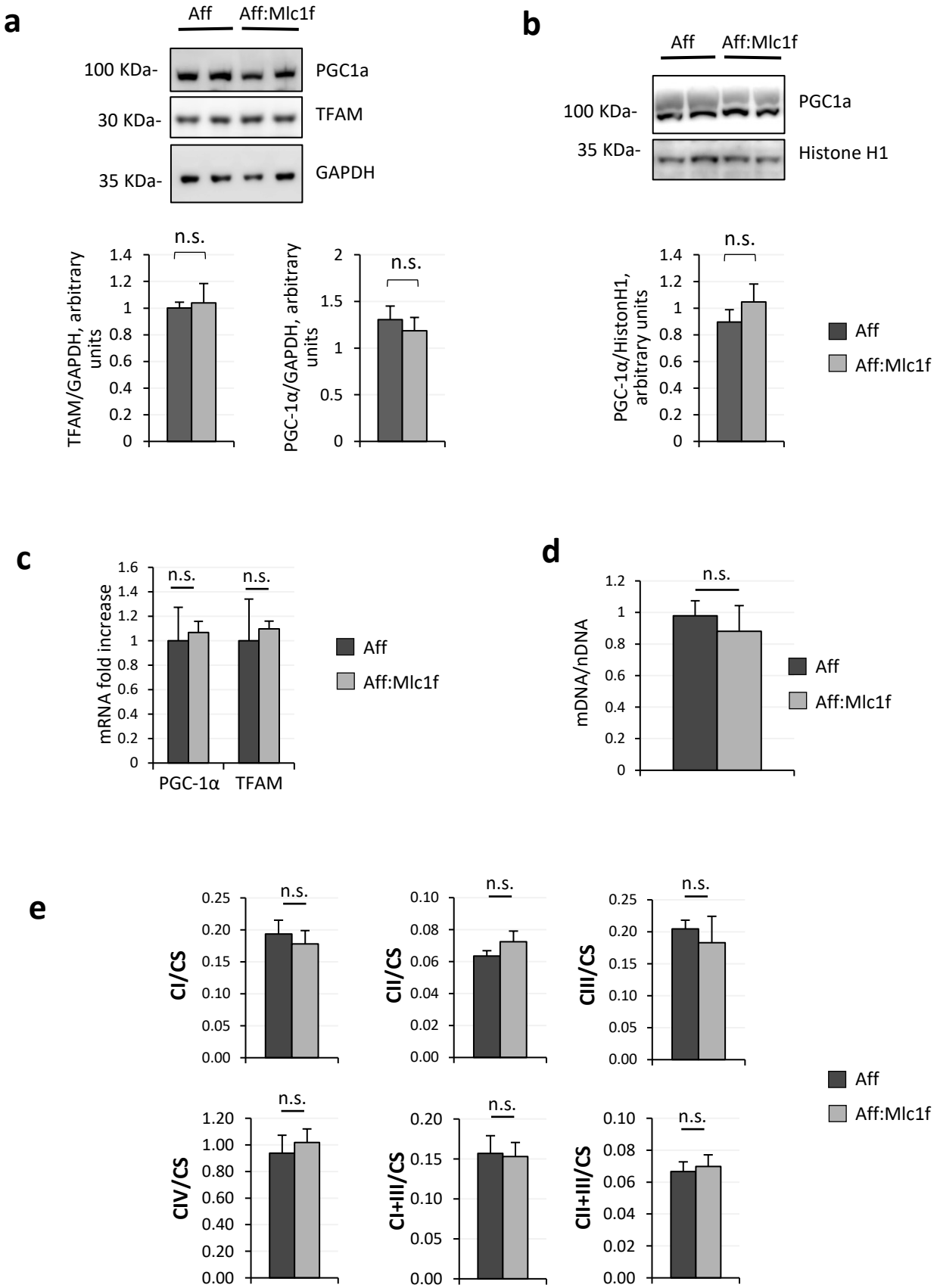

Supplementary Figure S3. Investigate mitochondria in muscles lacking Ambra1. (**a**) Western blotting for PGC-1α and TFAM in total protein extract of quadriceps muscle from 6-month-old *Ambra1*$^{f/f}$ (Aff) and *Ambra1*$^{f/f}$:*Mlc1f*-Cre (Aff:Mlc1f-Cre) mice. GAPDH was used as loading control. Densitometric quantifications of PGC-1α vs GAPDH and of TFAM vs GAPDH are shown on the bottom panels. Data are provided as mean±s.e.m. (*n* = 5-6 mice, each genotype n.s., not significant). (**b**) Western blotting for PGC-1α in nuclear fraction protein extract from quadriceps muscle of 6-month-old *Ambra1*$^{f/f}$ (Aff) and *Ambra1*$^{f/f}$:*Mlc1f*-Cre (Aff:Mlc1f-Cre) mice. Histone-H1 was used as loading control. Densitometric quantifications of PGC-1α vs Histone-H1 are shown on the bottom panel. Data are provided as mean±s.e.m. (*n* = 5-6 mice, each genotype; n.s., not significant). (**c**) Quantitative RT-PCR for PGC-1α and TFAM transcripts in quadriceps muscle of 6-month-old *Ambra1*$^{fl/fl}$ (Aff) and *Ambra1*$^{fl/fl}$:*Mlc1f*-Cre (Aff:Mlc1f) mice. Data are shown as mean±s.e.m. (*n* = 6-7 mice, each genotype; n.s., not significant). (**d**) Quantitative PCR for mitochondrial DNA (mDNA), normalized on nuclear DNA (nDNA), in quadriceps muscle of 6-month-old *Ambra1*$^{fl/fl}$ (Aff) and *Ambra1*$^{fl/fl}$:*Mlc1f*-Cre (Aff:Mlc1f) mice. Data are shown as mean±s.e.m. (*n* = 4 mice, each genotype; n.s., not significant). (**e**) Quantification of the activity of respiratory chain complex I (CI), complex II (CII), complex III (CIII), complex IV (CIV), complex I+III (SCI+III) and complex II+III (SCII+III) in mitochondria isolated from quadriceps muscles of sedentary 6-month-old *Ambra1*$^{fl/fl}$ (Aff) and *Ambra1*$^{fl/fl}$:*Mlc1f*-Cre (Aff:Mlc1f) mice. The activity of the different complexes was normalized on citrate synthase (CS) activity. Data are shown as mean±s.e.m. (*n* = 4 mice, each genotype; n.s., not significant).

Supplementary References

S1. Simoneschi D, Rona G, Zhou N, Jeong Y-T, Jiang S, Milletti G et al. CRL4AMBRA1 is a master regulator of D-type cyclins. *Nature* 2021;**592**:789–793.

S2. di Rienzo M, Romagnoli A, Ciccosanti F, Refolo G, Consalvi V, Arena G et al. AMBRA1 regulates mitophagy by interacting with ATAD3A and promoting PINK1 stability. *Autophagy* 2021;Nov **13**:1-11

S3. di Rita A, Peschiaroli A, D'Acunzo P, Strobbe D, Hu Z, Gruber J et al. HUWE1 E3 ligase promotes PINK1/PARKIN-independent mitophagy by regulating AMBRA1 activation via IKKα. *Nature Communications* 2018;**9**:1–18.

S4. Skarnes WC, Rosen B, West AP, Koutsourakis M, Bushell W, Iyer V et al. A conditional knockout resource for the genome-wide study of mouse gene function. *Nature* 2011;**474**:337–342.

S5. Eakin GS, Hadjantonakis A-K. Production of chimeras by aggregation of embryonic stem cells with diploid or tetraploid mouse embryos. *Nature Protocols* 2006;**1:**1145–1153.

S6. Rodríguez CI, Buchholz F, Galloway J, Sequerra R, Kasper J, Ayala R et al. High-efficiency deleter mice show that FLPe is an alternative to Cre-loxP. *Nature Genetics* 2000;**25**:139–140.

S7. Sakai K, Miyazaki JI. A transgenic mouse line that retains Cre Recombinase activity in mature oocytes irrespective of the Cre transgene transmission. *Biochemical and Biophysical Research Communications* 1997;**237**:318–324.

S8. Bothe GWM, Haspel JA, Smith CL, Wiener HH, Burden SJ. Selective expression of Cre Recombinase in skeletal muscle fibers. *genesis* 2000;**26**:165–166.

S9. Chrisam M, Pirozzi M, Castagnaro S, Blaauw B, Polishchuck R, Cecconi F et al. Reactivation of autophagy by spermidine ameliorates the myopathic defects of collagen VI-null mice. *Autophagy* 2015;**11**:2142.

S10. Rocchi A, He C. Activating autophagy by aerobic exercise in mice. *JoVE* 2017;2017:e55099.

S11. Milan G, Romanello V, Pescatore F, Armani A, Paik J-H, Frasson L et al. Regulation of autophagy and the ubiquitin–proteasome system by the FoxO transcriptional network during muscle atrophy. *Nature Communications* 2015;**6**:1–14.

S12. Metti S, Gambarotto L, Chrisam M, Baraldo M, Braghetta P, Blaauw B et al. The polyphenol ameliorates the myopathic phenotype of Collagen VI deficient mice via autophagy induction. *Frontiers in Cell and Developmental Biology* 2020;**8**:997.

S13. Schindelin J, Arganda-Carreras I, Frise E, Kaynig V, Longair M, Pietzsch T et al. Fiji: an open-source platform for biological-image analysis. *Nature Methods* 2012;**9**:676–682.

S14. Rizk A, Paul G, Incardona P, Bugarski M, Mansouri M, Niemann A et al. Segmentation and quantification of subcellular structures in fluorescence microscopy images using Squassh. *Nature Protocols* 2014;**9**:586–596.

S15. Encarnacion-Rivera L, Foltz S, Hartzell HC, Choo H. Myosoft: An automated muscle histology analysis tool using machine learning algorithm utilizing FIJI/ImageJ software. *PlOS One* 2020;15:e0229041

S16. Dimauro I, Pearson T, Caporossi D, Jackson MJ. A simple protocol for the subcellular fractionation of skeletal muscle cells and tissue. *BMC Research Notes* 2012;**5**:1–5.

S17. Spinazzi M, Casarin A, Pertegato V, Salviati L, Angelini C. Assessment of mitochondrial respiratory chain enzymatic activities on tissues and cultured cells. *Nature Protocols* 2012;**7**:1235–1246.

S18. Patro R, Duggal G, Love MI, Irizarry RA, Kingsford C. Salmon provides fast and bias-aware quantification of transcript expression. *Nature Methods* 2017;**14**:417–419.

S19. Maiani E, Milletti G, Cecconi F. The pro-autophagic protein AMBRA1 coordinates cell cycle progression by regulating CCND (cyclin D) stability. *Autophagy* 2021**;17:**4506-4508